Applied Physics Letters ARTICLE scitation.org/journal/apl

High electron mobility with significant spin-orbit coupling in rock-salt YbO epitaxial thin film

Cite as: Appl. Phys. Lett. **114**, 162104 (2019); doi: 10.1063/1.5085938
Submitted: 17 December 2018 · Accepted: 10 March 2019 ·
Published Online: 26 April 2019

View Online Export Citation CrossMark

Taku Yamamoto,[1] Kenichi Kaminaga,[2] Daichi Saito,[1] Daichi Oka,[1] and Tomoteru Fukumura[1,2,3,4,a)]

AFFILIATIONS

[1]Department of Chemistry, Graduate School of Science, Tohoku University, Sendai 980-8578, Japan
[2]WPI Advanced Institute for Materials Research and Core Research Cluster, Tohoku University, Sendai 980-8577, Japan
[3]Center for Science and Innovation in Spintronics (Core Research Cluster), Organization for Advanced Studies, Tohoku University, Sendai 980-8577, Japan
[4]Center for Spintronics Research Network, Tohoku University, Sendai 980-8577, Japan

[a)]Electronic mail: tomoteru.fukumura.e4@tohoku.ac.jp

ABSTRACT

We studied the optical and electrical properties of ytterbium monoxide (YbO) epitaxial thin films with unusual Yb^{2+} ($4f^{14}5d^0$) valence grown by the pulsed laser deposition method. The narrow bandgap of 0.25 eV and the large crystal field splitting of 5d orbitals in YbO determined from absorption spectra were consistent with the chemical trends of ytterbium monochalcogenides (Yb*Ch*s). Electrical resistivity was tunable upon electron doping via introduction of oxygen vacancies. Electron mobility at room temperature increased up to $\sim 13\ cm^2\ V^{-1}\ s^{-1}$ with increasing electron carrier density. The heavily electron-doped YbO showed weak antilocalization at low temperature, suggesting significant spin-orbit coupling owing to the heavy Yb nucleus.

Published under license by AIP Publishing. https://doi.org/10.1063/1.5085938

Rare earth elements (*RE*: Sc, Y, and lanthanides) usually prefer the trivalent ionic state to form the most stable binary sesquioxides RE_2O_3, which are well-known high permittivity wide-gap insulators promising for gate insulators.[1–3] For metastable rare earth monoxides (*RE*Os), on the other hand, the electronic properties are significantly different from those of RE_2O_3 because of the presence of nd (n = 3, 4, or 5) conduction carriers in addition to the localized 4f electrons around the Fermi energy.[4] Despite the promising potential of *RE*Os as electronic materials, their synthesis has been difficult because of much higher stability of RE_2O_3 than *RE*O except for EuO,[5] which is a well-known narrow-gap ferromagnetic semiconductor.[6] So far, several *RE*O (*RE* = La, Ce, Pr, Nd, and Sm) polycrystals have been synthesized under high pressure without sufficient investigation of their fundamental properties.[7–9] Recently, we succeeded in the growth of *RE*O epitaxial thin films by utilizing the non-equilibrium process of the pulsed laser deposition (PLD) method under ultrahigh vacuum. As a result, various functionalities were unveiled such as semiconducting electrical conduction in YO[10] and LuO,[11] superconductivity in LaO,[12] heavy-fermionic behavior in SmO,[13] and itinerant ferromagnetism in NdO.[14]

Previously, YbO polycrystalline powders were synthesized in a high pressure[15] and CO atmosphere,[16] and an YbO epitaxial film was grown on GaN.[17] In these studies, only a bandgap (E_g) of about 0.32 eV was estimated,[15] while YbO was theoretically predicted to be a band insulator with an electronic configuration of [Xe] $4f^{14}5d^0$ for Yb^{2+}.[18] Considering the narrow bandgap and the strong shielding effect of the fully occupied 4f band, YbO is expected to show high electrical conductivity by electron doping in the 5d conduction band. In this study, single crystalline YbO epitaxial thin films were grown in order to study the optical and electrical properties of YbO. In addition to the detailed optical absorption spectrum, high and tunable electrical conduction with high electron mobility was observed at room temperature. Furthermore, weak antilocalization (WAL) behavior was observed at low temperature, indicating significant spin-orbit coupling in YbO, promising for heteroepitaxial spintronic devices.

YbO epitaxial thin films were grown by PLD. The Yb metal (99.9%) target at a distance of 5 cm from the substrate was irradiated by the KrF excimer laser ($\lambda = 248$ nm) in an ultrahigh vacuum chamber with a base pressure of $\sim 10^{-9}$ Torr. Thin films were grown on $YAlO_3$ (110) and CaF_2 (111) substrates typically at 250 °C with a laser energy of 1.6 J/cm^2 and a pulse rate of 10 Hz. Oxygen partial pressure during growth (P_{O_2}) was monitored using a quadrupole mass spectrometer and controlled in the range of $2–5 \times 10^{-7}$ Torr by introducing pure O_2 gas. Samples A–D were grown on $YAlO_3$ (110) substrates at P_{O_2} values of 4.9×10^{-7}, 4.5×10^{-7}, 3.0×10^{-7}, and

2.0×10^{-7} Torr, respectively, for electrical measurements, where a laser energy of 0.8 J/cm^2 and a pulse rate of 20 Hz were used for sample D to introduce more oxygen vacancies. The film thickness decreased with decreasing P_{O_2} from samples A to D due to the high vapor pressure of the Yb metal (Table S1). In order to prevent the film oxidation, the amorphous AlO_x layer (~8 nm) was *in situ* deposited on the film surfaces at room temperature. The crystal structure was characterized by x-ray diffraction (XRD) by using a four-axis diffractometer (D8 Discover, Bruker AXS). The film thickness was measured using x-ray reflection or a stylus profilometer (ET 4000A, Kosaka laboratory ltd.). Optical transmittance and reflectance were measured for a YbO thin film on the CaF_2 (111) substrate by using Fourier transform infrared and ultraviolet-visible-near-infrared spectrometers (FT/IR-6600 and V-770, JASCO) because of negligible phonon absorption of CaF_2 in the measurement range. Optical absorption coefficient α was calculated by using the equation $\alpha = -\frac{1}{t}\ln\frac{T}{1-R}\frac{1-R_s}{T_s}$ (t is the film thickness, and T, R, T_s, and R_s are the transmittance and reflectance of the sample and the CaF_2 substrate, respectively). Electrical properties were evaluated for Hall-bar shaped thin films (Fig. S1) on the $YAlO_3$ (110) substrate by four-probe and Hall measurements using a measurement system (PPMS, Quantum Design).

Figure 1(a) shows the XRD θ–2θ pattern of the YbO thin film on the $YAlO_3$ (110) substrate (sample A). The peaks at $2\theta = 36.78°$ and 78.30° were rock-salt YbO 002 and 004 diffractions, respectively, without any impurity peak. A spotty peak of 224 diffraction in reciprocal space mapping indicated the epitaxial growth of the YbO thin film [Fig. 1(b)]. The epitaxial relationship was YbO (001) || $YAlO_3$ (110) and YbO [110] || $YAlO_3$ [001] as schematically shown in Fig. 1(c),

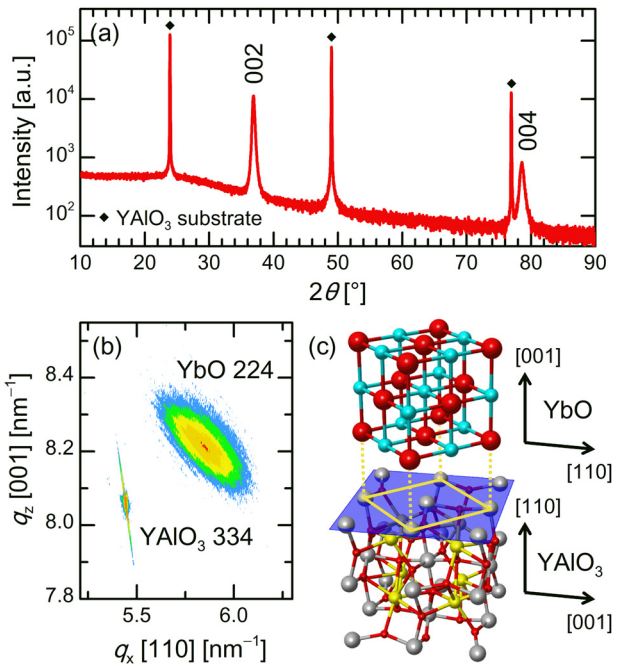

FIG. 1. (a) XRD θ–2θ pattern of the YbO (001) epitaxial thin film on the $YAlO_3$ (110) substrate (sample A). (b) Reciprocal space map around YbO 224 diffraction of the thin film. (c) Schematic image of the epitaxial relationship between the YbO epitaxial thin film and the $YAlO_3$ substrate.[30]

similar to the other rare-earth monoxide thin films on $YAlO_3$.[12,13,19] The thin film possessed lattice constants of $a = 4.83$ Å and $c = 4.87$ Å, whose values are close to those of the bulk polycrystal, $a = 4.88$ Å.[15] All the samples in this study were almost fully relaxed from the substrate (Table S1) due to the large lattice mismatch of ~7% between YbO and $YAlO_3$. The full width at half maximum of the rocking curve for 002 diffraction of sample A was 1.62°, while that for 111 diffraction of the (111) epitaxial thin film on the CaF_2 (111) substrate was improved to be 0.87° in spite of the large lattice mismatch of ~11%, yielding better crystallinity than the previously reported YbO (111) thin film on the GaN (0001) surface with the full width at half maximum of 1.77°.[17]

The absorption coefficient spectrum of the YbO (111) thin film on the CaF_2 (111) substrate, with carrier density similar to that of sample A (Table S1), is shown in Fig. 2(a). Three absorption peaks at $E_1 = 1.23$ eV, $E_2 = 2.70$ eV, and $E_3 > 5.5$ eV could be attributed to electron transfers from 4f to 5d t_{2g} (E_1), from 4f to 5d e_g (E_2), and from 2p to 5d t_{2g} (E_3), respectively, in analogy with the other Yb*Ch*s[20] [Fig. 2(c)]. The Tauc plot around the absorption edge in the inset of Fig. 2(a) indicated indirect transition, which is consistent with the theoretical band structure.[18] Also, E_g of 0.25 eV determined from the intercept of the fitting line [inset of Fig. 2(a)] was comparable to the value of 0.32 eV estimated from the high pressure study.[15] These results confirmed that YbO is an intrinsic narrow-gap semiconductor. For another YbO with higher oxygen vacancies grown under low P_{O_2}, the energy levels E_1–E_3 were unshifted, while the band edge was hidden

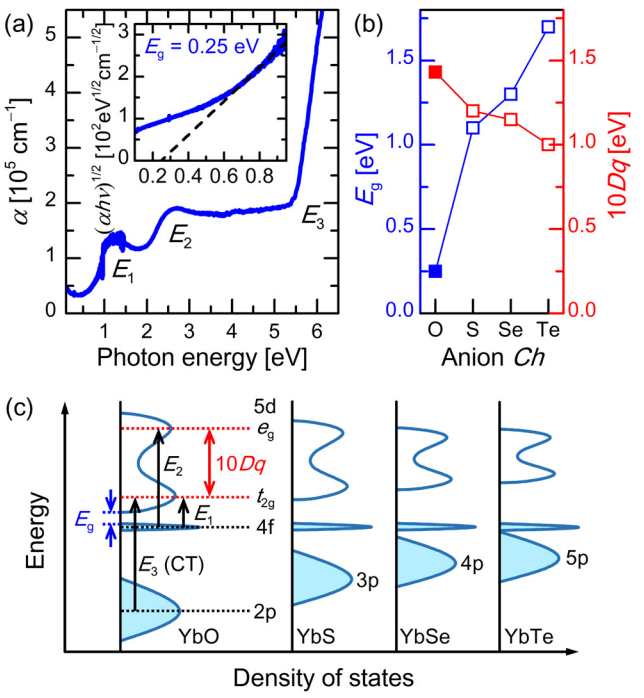

FIG. 2. (a) Absorption coefficient spectrum of the YbO (111) epitaxial thin film on the CaF_2 (111) substrate. The inset shows the Tauc plot for the absorption edge. (b) Chemical trends of the bandgap and crystal field splitting in Yb*Ch*s [*Ch* = O (solid square), S, Se, and Te (open square)[6,20,21]]. (c) Schematic energy diagrams for band structures in Yb*Ch*s. CT denotes the charge transfer.

Published under license by AIP Publishing

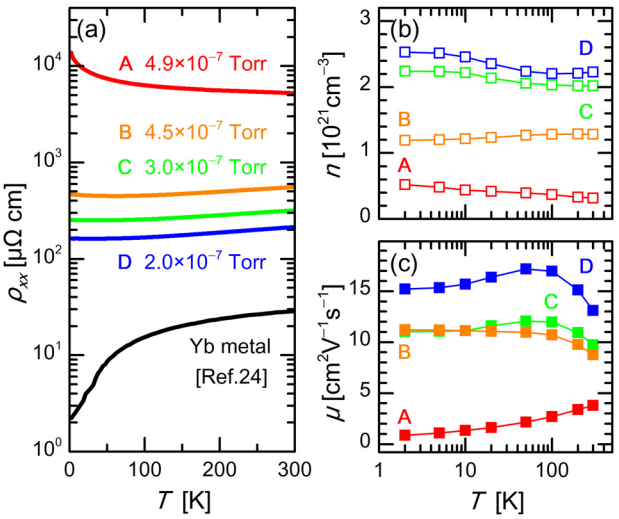

FIG. 3. Temperature dependence of (a) electrical resistivity, (b) electron density, and (c) electron mobility for YbO epitaxial thin films grown at different P_{O_2} values denoted in (a). Resistivity for the Yb metal is also shown in (a) for reference.[24]

by significant free electron absorption (Fig. S2). This result justifies the rigid-band-like picture of YbO in this study. The chemical trends of crystal field splitting ($10Dq$) and E_g evaluated for Yb*Ch*s in Fig. 2(b)[6,20,21] showed systematic variation upon decreasing the period of *Ch* from Te to O. The decrease in E_g between 5d and 4f bands could be attributed to the increase in $10Dq$ caused by the more ionic character of the lighter *Ch*s as well as smaller hybridization between 5d and np (n = 2, 3, 4, 5) bands [Fig. 2(c)]. These trends in the band structure were also reported for other Sm*Ch*s[13,22] and Eu*Ch*s.[23]

The temperature T dependence of electrical resistivity ρ_{xx} of the samples A–D grown at different P_{O_2} values and in the hcp-Yb metal[24] is shown in Fig. 3(a). The YbO thin films showed one or two decade higher resistivity in contrast to the Yb metal. Upon decreasing P_{O_2}, the resistivity decreased monotonically from insulating ($d\rho_{xx}/dT < 0$ in sample A) to metallic ($d\rho_{xx}/dT > 0$ in samples B–D) conduction. At the low temperatures, the conductivity (σ_{xx}) of samples A and B showed log T-linear behavior, corresponding to weak localization as seen in Fig. 4, while σ_{xx} of the samples C and D was almost T-independent (Fig. S3). The observed local resistivity minimum also suggests a possibility of the Kondo effect, as was reported in SmO.[13]

Nearly temperature independent electron carrier density n increased monotonically from samples A to D with decreasing P_{O_2} [Fig. 3(b)], implying that oxygen vacancies served as an electron donor like ordinary oxide semiconductors. On the other hand, electron mobility μ increased monotonically with increasing n [Fig. 3(c)], with the highest value of 17 $cm^2V^{-1}s^{-1}$ at 50 K and 13 $cm^2V^{-1}s^{-1}$ at 300 K for sample D. It is noted that similar mobility of the sample on CaF_2 (111) (Table S1) corroborates intrinsically high mobility of YbO. The mobility at room temperature was the highest among ever reported *RE*Os[10,12,25] except for EuO.[26] The extraordinarily high mobility of YbO probably originated from the fully occupied 4f orbital with a spherical charge distribution which strongly screens the Yb nucleus charge from electron trapping.

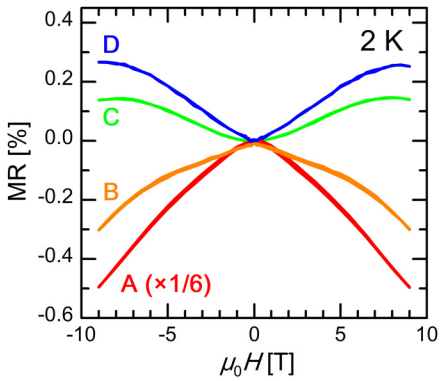

FIG. 4. Magnetoresistance for YbO epitaxial thin films (samples A–D) at 2 K under an out-of-plane magnetic field.

Figure 4 shows magnetoresistance (MR) of samples A–D at 2 K. While samples A and B showed negative MR, samples C and D with higher n exhibited cusp-like positive MR. Such MR was observed in heavily electron-doped YO[10] and LuO,[11] as was attributed to the weak antilocalization (WAL) effect. Generally, the depth of the cusp in WAL is a monotonically increasing function of the ratio of phase coherence time to spin coherence time. The enhanced WAL in YbO with increasing n is reminiscent of large spin-orbit coupling narrow-gap semiconductors such as InSb[27] and is consistent with the theoretical predictions that the upper shift of Fermi energy enhances spin-orbit coupling, resulting in shorter spin coherence time.[28,29] The WAL behavior in the heavily doped YbO suggests significant spin-orbit coupling caused by the heavy element Yb.

In summary, rock-salt YbO (001) and (111) epitaxial thin films on $YAlO_3$ (110) and CaF_2 (111) substrates were grown by the pulsed laser deposition method, respectively. YbO was found to be a narrow-gap semiconductor with the bandgap of 0.25 eV and showed a variable electrical conduction by electron doping with a remarkably high electron mobility of 13 $cm^2V^{-1}s^{-1}$ at room temperature. The observed weak antilocalization behavior suggests significant spin-orbit coupling originating from the large mass of Yb. The high conductivity concomitant with spin-orbit coupling is promising for spin-charge conversion in heteroepitaxial spintronic devices.

See supplementary material for Hall-bar pattern geometry, optical absorption spectra, electrical conductivity, and experimental parameters of YbO epitaxial thin films in this study.

We thank Y. Matsumoto, S. Maruyama, and R. Kumashiro of Tohoku University for technical assistance. This work was supported by MEXT/JSPS (18H03872, 26105002) and the Mitsubishi Foundation.

REFERENCES

[1]M. Mikami and S. Nakamura, J. Alloys Compd. **408–412**, 687 (2006).
[2]M. Leskelä, K. Kukli, and M. Ritala, J. Alloys Compd. **418**, 27 (2006).
[3]C. D. Wilk, J. Appl. Phys. **89**, 5243 (2001).
[4]G. Adachi and N. Imanaka, Chem. Rev. **98**, 1479 (1998).
[5]J. M. Leger, N. Yacoubi, and J. Loriers, J. Solid State Chem. **36**, 261 (1981).
[6]M. Mauger and C. Godart, Phys. Rep. **141**, 51 (1986).
[7]J. M. Leger, P. Aimonino, J. Loriers, P. Dordor, and B. Coqblin, Phys. Lett. A **80**, 325 (1980).

Published under license by AIP Publishing

[8]G. Krill, M. F. Ravet, J. P. Kappler, L. Abadli, J. M. Leger, N. Yacoubi, and C. Loriers, Solid State Commun. **33**, 351 (1980).
[9]I. Vedel, A. M. Redon, and J. M. Leger, Solid State Phys. **19**, 3549 (1986).
[10]K. Kaminaga, R. Sei, K. Hayashi, N. Happo, H. Tajiri, D. Oka, T. Fukumura, and T. Hasegawa, Appl. Phys. Lett. **108**, 122102 (2016).
[11]K. Kaminaga, D. Oka, T. Hasegawa, and T. Fukumura, ACS Omega **3**, 12501 (2018).
[12]K. Kaminaga, D. Oka, T. Hasegawa, and T. Fukumura, J. Am. Chem. Soc. **140**, 6754 (2018).
[13]Y. Uchida, K. Kaminaga, T. Fukumura, and T. Hasegawa, Phys. Rev. B **95**, 125111 (2017).
[14]D. Saito, K. Kaminaga, D. Oka, and T. Fukumura, "Itinerant ferromagnetism in rocksalt NdO epitaxial thin films," (submitted).
[15]A. Werner, H. D. Hochheimer, A. Jayaraman, and J. M. Leger, Solid State Commun. **38**, 325 (1981).
[16]A. Goto, Y. Ohta, and M. Kitamura, J. Mater. Sci. Chem. Eng. **6**, 85 (2018).
[17]M. D. Losego, S. Mita, R. Collazo, Z. Sitar, and J. P. Maria, J. Cryst. Growth **310**, 51 (2008).
[18]Z. Li and J. Zhang, J. Phys. Soc. Jpn. **84**, 054706 (2015).
[19]R. W. Ulbricht, A. Schmehl, T. Heeg, J. Schubert, and D. G. Schlom, Appl. Phys. Lett. **93**, 102105 (2008).
[20]V. Narayanamurti, A. Jayaraman, and E. Bucher, Phys. Rev. B **9**, 2521 (1974).
[21]R. Suryanarayanan, J. Ferré, and B. Briat, Phys. Rev. B **9**, 554 (1974).
[22]B. Batlogg, E. Kaldis, A. Schlegel, and P. Wachter, Phys. Rev. B **14**, 5503 (1976).
[23]K. A. Gschneider, Jr. and L. Eyring, *Handbook on the Physics and Chemistry of Rare Earths* (North Holland, Amsterdam, 1979), Vol. 2.
[24]M. A. Curry, S. Legvold, and F. H. Spedding, Phys. Rev. **117**, 953 (1960).
[25]Y. Uchida, Master thesis, The University of Tokyo, 2016.
[26]Y. Shapira, S. Foner, and T. B. Reed, Phys. Rev. B **8**, 2299 (1973).
[27]R. L. Kallaher and J. J. Heremans, Phys. Rev. B **79**, 075322 (2009).
[28]R. J. Elliott, Phys. Rev. **96**, 266 (1954).
[29]M. I. Dyakonov and V. I. Perel, Phys. Lett. A **35**, 459 (1971).
[30]K. Momma and F. Izumi, J. Appl. Crystallogr. **44**, 1272 (2011).

Published under license by AIP Publishing